DEVELOPMENTAL DYNAMICS 244:1259–1275, 2015
DOI: 10.1002/DVDY.24309

RESEARCH ARTICLE

MiR-23b and miR-199a Impair Epithelial-to-Mesenchymal Transition During Atrioventricular Endocardial Cushion Formation

Fernando Bonet,[1] Ángel Dueñas,[1] Carmen López-Sánchez,[2] Virginio García-Martínez,[2] Amelia E. Aránega,[1] and Diego Franco[1]*

[1]Cardiovascular Research Group, Department of Experimental Biology, Faculty of Experimental Sciences, University of Jaén, Jaén, Spain
[2]Department of Anatomy and Embryology, Faculty of Medicine, University of Extremadura, Badajoz, Spain

Background: Valve development is a multistep process involving the activation of the cardiac endothelium, epithelial-mesenchymal transition (EMT) and the progressive alignment and differentiation of distinct mesenchymal cell types. Several pathways such as Notch/delta, Tgf-beta and/or Vegf signaling have been implicated in crucial steps of valvulogenesis. We have previously demonstrated discrete changes in microRNAs expression during cardiogenesis, which are predicted to target Bmp- and Tgf-beta signaling. We now analyzed the expression profile of 20 candidate microRNAs in atrial, ventricular, and atrioventricular canal regions at four different developmental stages. Results: qRT-PCR analyses of microRNAs demonstrated a highly dynamic and distinct expression profiles within the atrial, ventricular, and atrioventricular canal regions of the developing chick heart. miR-23b, miR-199a, and miR-15a displayed increased expression during early AVC development whereas others such as miR-130a and miR-200a display decreased expression levels. Functional analyses of miR-23b, miR-199a, and miR-15a overexpression led to in vitro EMT blockage. Molecular analyses demonstrate that distinct EMT signaling pathways are impaired after microRNA expression, including a large subset of EMT-related genes that are predicted to be targeted by these microRNAs. Conclusions: Our data demonstrate that miR-23b and miR-199a over-expression can impair atrioventricular EMT. *Developmental Dynamics 244:1259–1275, 2015*. © 2015 Wiley Periodicals, Inc.

Key words: miR-23b; miR-199a; EMT; cardiac valve development

Submitted 19 January 2015; Last Decision 15 June 2015; Accepted 15 June 2015; Published online 21 July 2015

Introduction

Valvular heart disease is a major cause of morbidity and mortality in the adult human population (American Heart Association, 2004). Importantly, congenital valve anomalies as well as a large subset of adult valve diseases originate as a consequence of abnormal embryonic development (Hinton et al., 2006, 2008; Hinton and Yutzey, 2011; Lincoln et al., 2004; Lincoln and Yutzey, 2011; Wirrig and Yutzey, 2011; Markwald et al., 2011).

Valve development is a multistep process highly conserved among different vertebrate species. A series of temporally concatenated events occur during valve morphogenesis, starting with endocardial activation, epithelial-mesenchymal transition (EMT), differentiation of distinct mesenchymal cell types, and remodeling of endocardial cushion into the definitive valve morphology. Epithelial-mesenchymal transformation (EMT) constitutes a key developmental process during valve morphogenesis, which is finely-regulated (Thiery and Seelman, 2006). EMT requires active down-regulation of cell-cell adhesion molecules (i.e., cadherins), degradation of the basement membrane, and remodeling of the cytoskeleton leading to the loss of apicobasal cell polarity (Hay, 2005).

At the molecular level, a role for Notch signaling in the regulation of EMT has been thoroughly described (Timmerman et al., 2004; Westin and Lardelli, 1997). Notch signaling provides competence to endocardial cells to undergo EMT from specific areas of the heart-forming field before heart tube formation (Drake and Jacobson, 1988; Virágh et al., 1989; Linask and Lash, 1993), although alternative evidence suggests that such competence is conferred thereafter, only in a subset of endocardial cushion cells (Timmerman et al., 2004). After specification, Tgf-β signaling, through Snail/Slug results in decreased VE-cadherin expression, allowing endocardial cells to separate, thus activating the mesenchymal transdifferentiation programme (for a review see, Armstrong and Bischoff, 2004). Concomitantly with the delamination process, endocardial cells are repopulated by a VEGF-dependent process (Johnson et al., 2003; for a review see, Armstrong and Bischoff, 2004). Migratory behavior of differentiating mesenchymal cells is mediated in part by the composition of cardiac jelly, particularly hyaluronic acid (Camesnisch et al., 2004), which thus

Grant sponsor: Junta de Andalucía Regional Council; Grant numbers: CTS-1614 and CTS-03878; Grant sponsor: Junta de Extremadura Regional Council.
*Correspondence to: Diego Franco, Department of Experimental Biology B3-362, Faculty of Experimental Sciences, University of Jaén, 23071 Jaén, Spain. E-mail: dfranco@ujaen.es

Article is online at: http://onlinelibrary.wiley.com/doi/10.1002/dvdy.24309/abstract

constitutes a determinant factor shaping the remodeling steps of valve morphogenesis (Lincoln and Yutzey, 2011; Hinton and Yutzey, 2011). Valve morphogenesis is thus a complex developmental process in which distinct signaling pathways are intricately involved and interconnected.

MicroRNAs (miRNAs) are a class of small non-coding RNAs (19–25 nucleotides) that regulate gene expression by targeting complementary sequences of protein-encoding transcripts, eliciting thereafter translation blockage and/or mRNA degradation (Bernhart et al., 2006). A single miRNA is predicted to regulate multiple genes, thus modulating diverse biological processes (Doench and Sharp, 2004) as well as multiple steps within a single process (Canfran-Duque et al., 2014). Previous studies in our laboratory have demonstrated that microRNAs are dynamically expressed during ventricular chamber formation (Chinchilla et al., 2011). Curiously, our data revealed that differentially expressed microRNAs display increasing expression profiles during ventricular maturation. More recent studies have also demonstrated dynamic microRNA expression profiles during cardiac development (Synnergren et al., 2011; Zhou et al., 2014) as well as in left/right cardiac chambers (Vacchi-Suzzi et al. 2013). Yet to date only a handful of microRNAs have been functionally characterized. In this context, miR-1 serves as paradigm of important regulators during cardiac development (Zhao and Srivastava, 2007).

Over the last decade, a large body of evidence concerning the role of distinct microRNAs during EMT has been gained. These data have been obtained mainly in carcinogenesis, a process in which EMT also plays a highly relevant role (for a recent review, see Lamouille et al., 2013; Feng et al., 2014; Bouyssou et al., 2014; Diaz-Lopez et al., 2014). On the contrary, the functional role of microRNAs has been little studied during cardiac valve EMT. In this regard, miR-23 has been reported to be required to restrict endocardial cushion formation by inhibiting *Has2* expression and extracellular hyaluronic acid production in the embryonic heart (Lagendijk et al., 2011) and miR-21 plays a necessary role in cardiac valvulogenesis, through down-regulation of Pdcd4 (Kolpa et al., 2013) in zebrafish. In this study, we sought to obtain further insights into the functional role of differentially expressed microRNAs during atrioventricular EMT in the chick embryo.

Results

Differential microRNA Expression During Atrioventricular Canal Development in Chicken

microRNAs are widely and differentially expressed within the cardiovascular system, as recently reported (Synnergren et al., 2011; Chinchilla et al., 2011; Vacchi-Suzzi et al., 2013; Zhou et al., 2014). To obtain insights into the putative functional role of microRNAs during cardiac valvulogenesis, we have analyzed by qRT-PCR the endogenous expression level of 20 candidate microRNAs in the atrial, ventricular, and atrioventricular canal regions at different developmental stages, selected from those previously shown to be differentially expressed during cardiogenesis (Chinchilla et al., 2011). Our qRT-PCR analyses demonstrated a highly dynamic expression within the atrial, ventricular, and atrioventricular canal regions of the developing chick heart just before the onset of EMT (stage HH13) for most of the analyzed microRNAs (Fig. 1A–D). Two microRNAs (2/20; 10%; miR-27a and miR-206) are exclusively expressed in the ventricular chambers, two other microRNAs (2/20; 10%; miR-24, miR-133a) display similar expression in the AVC compared to the ventricles whereas four microRNAs (4/22; 20%; miR-1, miR-21, miR-31, and miR-92b) display similar expression levels in the AVC and atrial chambers (Fig. 1C). Thus, these microRNAs might therefore play a role in regulating chamber-specific expression. In addition, miR-15b (1/20; 5%) displays no significant differences among the distinct cardiac chambers, whereas three microRNAs (3/20; 15%; miR-140, miR-221 and miR-363) displayed differences within all cardiac chambers. Three other microRNAs (3/20; 15%, miR-27b, miR-153, miR-195) display no expression at all at HH13 stage, but two of three (miR-27b, miR-153) display differential expression at HH20 (Fig. 1D). We have focused our attention on those microRNAs that display differential expression in the AVC compared to atrial and ventricular chambers (5/20; 20%) (Fig. 1A,B). In this regard, three (3/20; 15%) microRNAs, i.e., miR-15a, miR-23b, and miR-199a, display increased expression levels in the AVC at HH13 compared to the atrial and ventricular chambers, suggesting a putative role in the onset of EMT (Fig. 1A). Curiously, miR-15a also displays increased AVC expression at HH20 and miR-23b and miR-199a at HH27 and HH31 (Fig. 1A), respectively, suggesting that it might play a role during subsequent stages of endocardial cushion remodeling. Importantly, miR-130a and miR-200a (2/22; ~9%) display decreased expression levels in the AVC at HH13 compared to the atrial and ventricular chambers (Fig. 1B). Similarly, these microRNAs display decreased expression levels at later developmental stages suggesting that they might also be required during subsequent atrioventricular valve development (Fig. 1B).

miR-15a, miR-23b and miR-199a, But Not miR-130a or miR-200a, Inhibit EMT

As previously stated, five distinct microRNAs display differential AVC expression at early developmental stages, suggesting a putative role in the EMT process. To determine the functional significance of these microRNAs, AV canal explants were cultured on collagen gels at the stage in which EMT is just starting (HH17) (Markwald et al., 1975, 1977; Bolender and Markwald, 1979), and transfected with the corresponding microRNA precursor for 24 hr. qRT-PCR analyses of pre-miRNA transfected explants nicely demonstrate a specific over-expression of the corresponding miRNA as illustrated in Figure 2A,B. Serial confocal image analyses of microRNA transfected and control explants, followed by quantitative analyses of the percentage of alpha-SMA positive cells (as a marker of differentiated mesenchymal cells; Scanlon et al., 2013), demonstrate that over-expression of miR-15a, miR-23b, and miR-199a significantly block the EMT process in a similar fashion to positive control explants treated with high glucose administration (Enciso et al., 2003) (Fig. 2C–K). Importantly, anti-miR-23b transfection reversed EMT phenotype as compared to pre-miR-23b treatment (Fig. 2C, J,K). On the other hand, miR-130a or miR-200a over-expression does not alter EMT process. No changes in the EMT process were observed in AVC explants treated with lipofectamine alone or transfected with scrambled negative controls, respectively (Fig. 2C). Thus, our data illustrate that miR-15a, miR-23b, and miR-199a can block in vitro EMT. It is important to highlight in this context that miR-23b and miR-199 exert a more robust EMT blockage than miR-15a (Fig. 2C). To further support a functional role of these microRNAs during EMT, LNA-based in situ hybridization experiments were carried out. MiR-15a and miR-199a ISH displayed very low expression levels in the developing heart, precluding the demonstration of

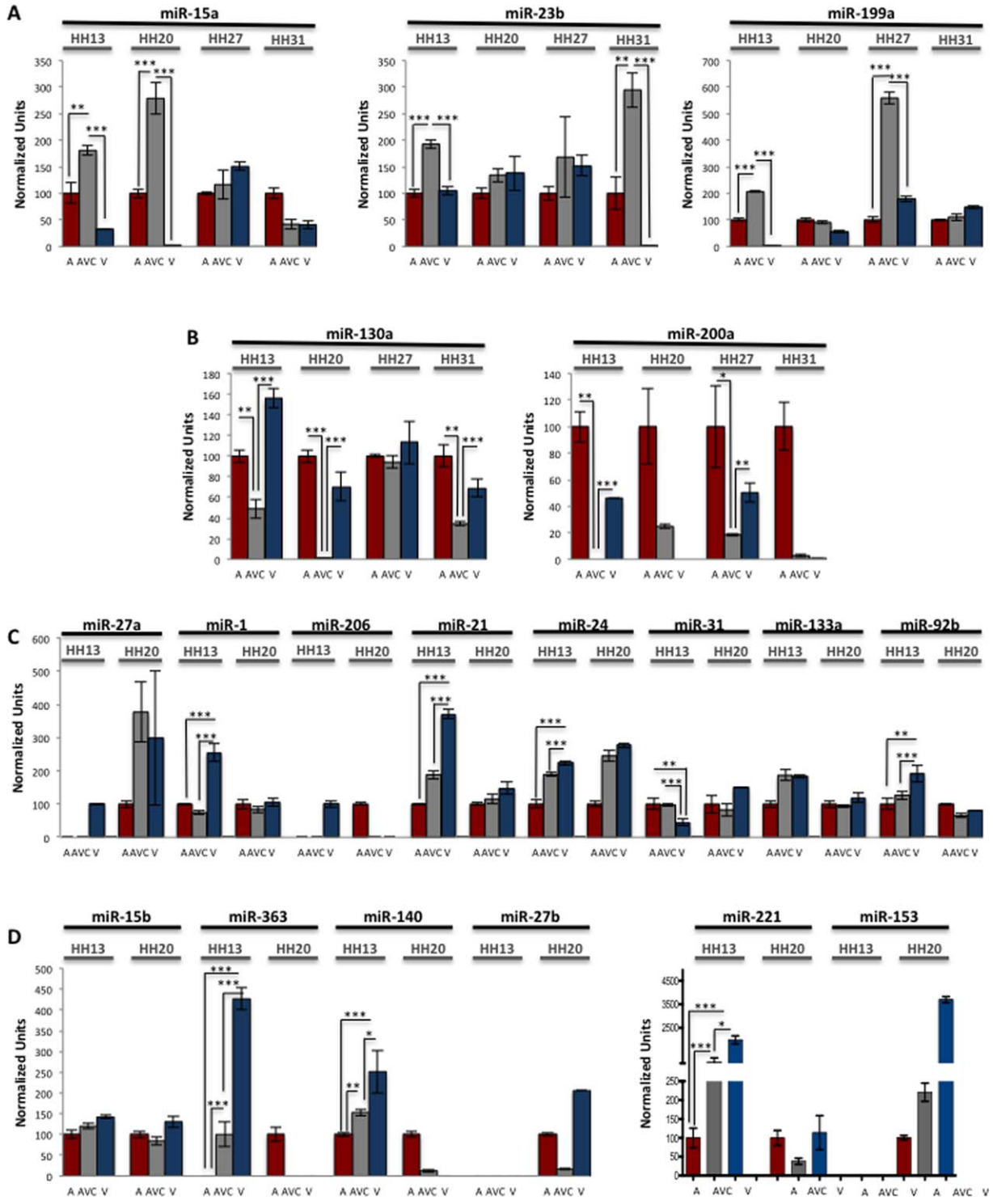

Fig. 1. microRNA expression profiles in distinct cardiac compartments at different chick developmental stages. **A, B:** qRT-PCR analyses of atrial, atrioventricular, and ventricular chambers illustrating the different expression profiles of miR-15a, miR-23b, miR-199a (A), miR-130a and miR-200a (B) at different developmental stages, i.e., HH13, HH20, HH27 and HH31 stages. miR-15a, miR-23b, and miR-199a display increased expression levels in AVC, whereas miR-130a and miR-200a display decreased expression levels in AVC at HH13 stage, compared to the atrial and ventricular regions. **C:** qRT-PCR analyses of atrial, atrioventricular and ventricular chambers illustrating different expression profile of miR-27a, miR-206, miR-24, miR-133a, miR-1, miR-21, miR-31, and miR-92 at HH13 and HH20 stages. miR-27a and miR-206 are exclusively expressed in the ventricular chamber at HH13 stage. miR-24 and miR-133a display similar expression in the AVC compared to the ventricles at HH13 stage. miR-1, miR-21, miR-31, and miR-92 display similar expression in the AVC compared to the atrial chambers at HH13 stage. **D:** qRT-PCR analyses of atrial, atrioventricular and ventricular chambers illustrating different expression profiles of miR-15b, miR-140, miR-221, miR-363, miR-27b, and miR-153 at HH13 and HH20 stages. miR-15b displays no significant differences among the distinct cardiac chambers, whereas miR-140, miR-221, and miR-363 display differences within all cardiac chambers at HH13 stage. miR-27b and miR-153 display no expression at all cardiac chambers at HH13 stage. Relative levels of expression were normalized using *5S* and *6U* as internal controls. * $P < 0.05$, ** $P < 0.01$, *** $P < 0.001$.

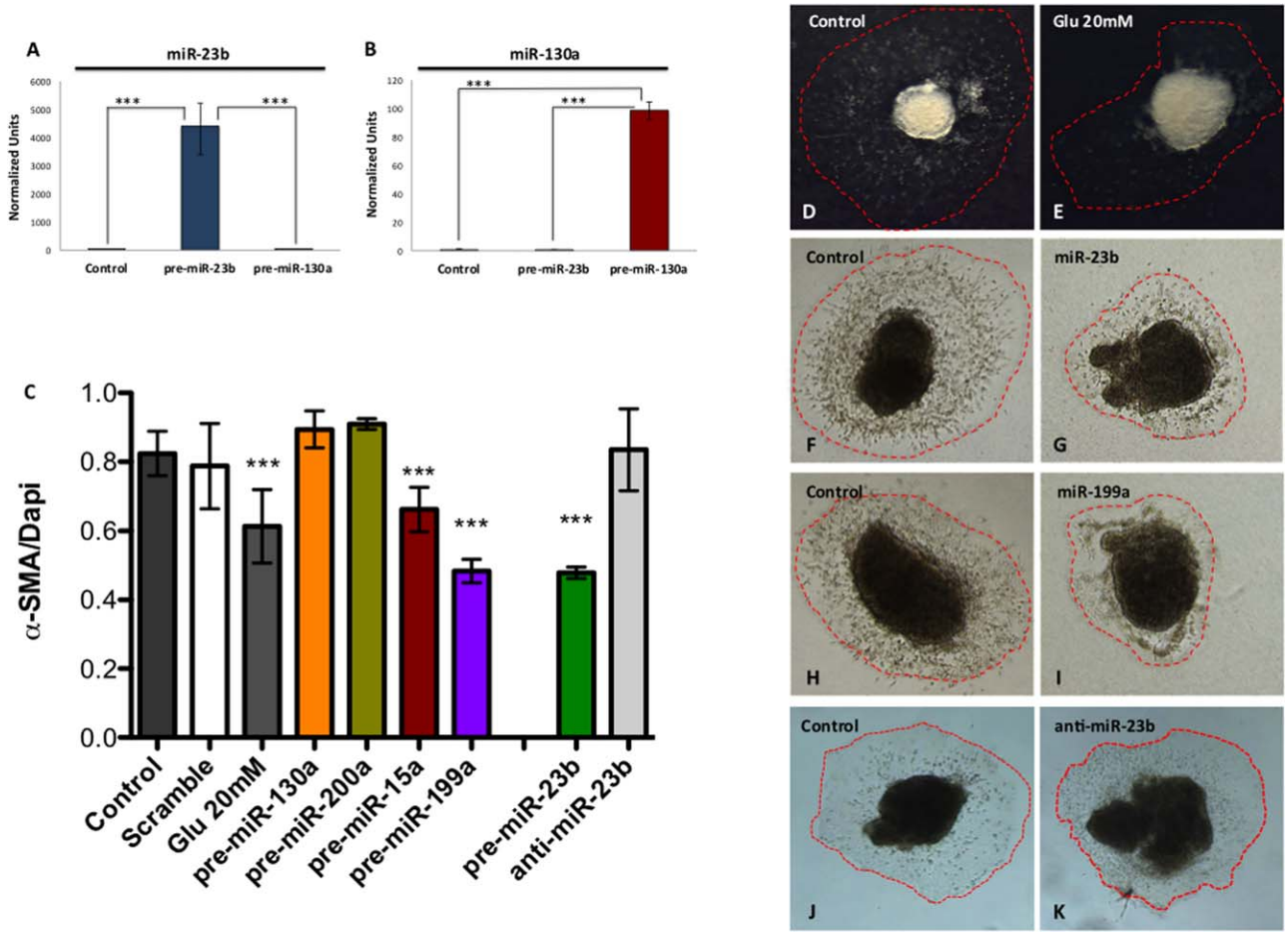

Fig. 2. miR-15a, miR-23b, and miR-199a block the EMT process in AVC explant cultures. **A, B:** qRT-PCR analyses demonstrate selective over-expression of miR-23b (A) and miR-130a (B) in AVC explants after pre-miRNAs transfection, respectively. **C:** Quantification of the percentage of EMT in control, glucose treated, pre-miRNA, and anti-miRNA transfected AVC explants after 24 hr of culture, respectively. As it can be observed, pre-miR-15a, pre-miR-23b and pre-miR-199a treatment, but not pre-miR-130a and pre-miR-200a, display lower EMT percentage compared to control and pre-miRNA scrambled conditions, in a similar fashion to high glucose administration control. Note also that anti-miR-23b treatment reversed the effects of pre-miR-23b over-expression. **D–K:** Representative microscopy images from AVC explant cultures incubated during 24 hr in control conditions (D,F,H, and J) and after pre-miRNA-23b (G), pre-miR-199a (I), and anti-miRNA-23b transfection (K), respectively. F corresponds to a positive control of EMT inhibition resulting from pre-incubation with Glucose (Glu) 20 mM. Note that Glu 20 mM, miR-23b and miR-199a conditions display lower EMT spreading compared to control conditions. Relative levels of expression were normalized using *5S* and *6U* as internal controls. * $P < 0.05$, ** $P < 0.01$, *** $P < 0.001$.

significant AVC differential expression by this method (data not shown). On the other hand, miR-23b ISH demonstrated enhanced expression of this microRNA in the developing valves as illustrated in Figure 3.

miR-23b and miR-199a Differentially Disrupt Key EMT Signaling Pathways Acting at Different Levels

Cardiac valve development is a highly dynamic developmental process in which four consecutive steps can be discerned, i.e., endocardial cell determination and specification, delamination and repopulation of these cells, transdifferentiation and migration into the extracellular matrix, and remodeling of endocardial cushions. Over the last decade, a large body of knowledge has been gained as to the distinct signaling pathways, such as Notch/delta, Tgf-beta/Bmp and Vegf, governing these processes (Westin and Lardelli, 1997; Yamagishi et al., 1999; Romano and Runyan, 2000; Miquerol et al., 2000; Dor et al., 2001; Kim et al., 2001; Gaussin et al., 2002; Johnson et al., 2003; Sugi et al., 2004; Timmerman et al., 2004). In order to investigate whether miR-15a, miR-23b and miR-199a disrupt distinct signaling pathways involved in the early stages of cardiac valvulogenesis, HH17 AVC explants cultured on collagen gels were transfected with microRNA precursors and expression analyses of candidate genes involved in distinct EMT steps were analyzed by qRT-PCR.

Recently, it has been demonstrated that Notch plays an essential role controlling EMT cell specification during endocardial cushion formation (Timmerman et al., 2004). qRT-PCR analyses demonstrated that *Notch1* expression is down-regulated after miR-23b and miR-199a over-expression, respectively, but not with miR-15a (Fig. 4A). These data suggest that miR-23b and miR-199a can modulate endocardial cell specification during atrioventricular EMT.

Multiple studies have provided substantial evidence on the important role of Tgf-beta/Bmp signaling, through complex Tgf-beta and Bmp receptor interaction (including Alk3, TgfbrI/rII,

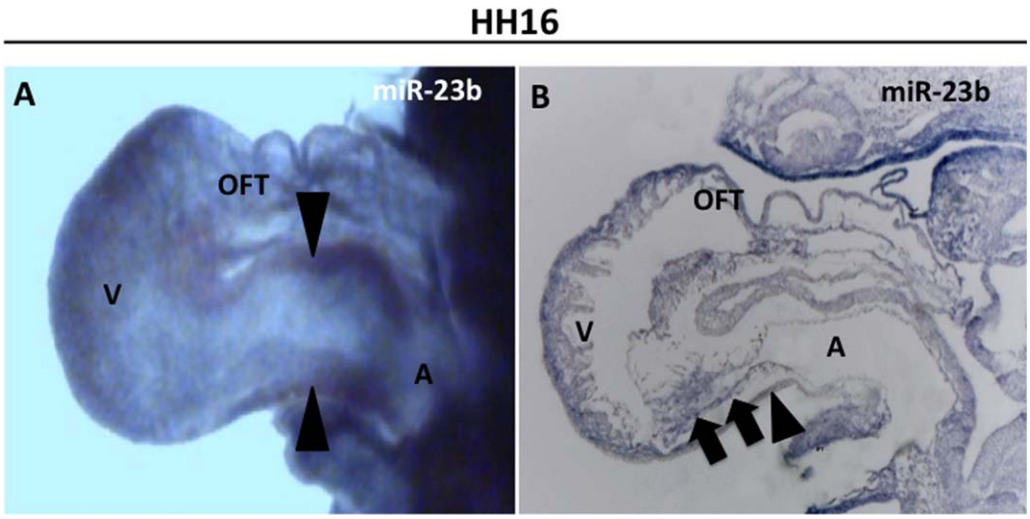

Fig. 3. LNA in situ hybridization for miR-23b in developing chicken heart. Representative images of whole-mount heart (**A**) and sagittal cardiac histological section (**B**) corresponding to LNA in situ hybridization against miR-23b in HH16 developing chicken hearts. Note that expression of miR-23b is enhanced in the AV region, displaying positive signal in both the myocardial (arrowhead) and mesenchymal (arrows) component of the atrioventricular canal. A, atria, OFT, outflow tract; IFT, inflow tract; V, ventricle.

and BmprII) and Smad activation, on the initiation of endocardial cell delamination and thus EMT progression (Nakajima et al., 2000; Hata et al., 1998). Synergy between Tgf-beta and Bmp signaling in cardiac cushion explants has been shown to facilitate EMT (Armstrong and Bischoff, 2004). Tgf-beta signaling leads to Snail/Slug transcription factor activation, which in turn destabilizes cell-cell contacts (VE-cadherin, i.e., *Chd5*) and promotes mesenchymal differentiation (alpha-SMA, i.e., *Acta2*).

Overexpression of miR-15a significantly up-regulates *Tgfbr1* and *Tgfbr2*, down-regulates *Smad6* while no changes were detected for *Snail*, *Cdh5,* or *Acta2* expression (Fig. 4B–G). miR-23b overexpression results in significant *Tgfbr1*, *Smad6*, *Snail,* and *Acta2* down-regulation whereas *Cdh5* expression is up-regulated (Fig. 4B–G). However, miR-199a over-expression leads to no significant changes in *Tgfbr1* and *Acta2* expression but up-regulation of *Tgfbr2* and *Cdh5* and down-regulation of *Smad6* and *Snail* (Fig. 4B–G). Thus, these data suggest that miR-15a, miR-23b, and miR-199a may modulate the delamination step during atrioventricular EMT process while only miR-23b seems to regulate the mesenchymal differentiation step.

Vegf signaling, through activation of Flt1 (*Vegfr1*) and Kdr (*Vegfr2*) receptors and Nfatc1 transcriptional activation, increases the endothelial valve proliferation and repopulation of the endocardial cells that have undergone EMT (Johnson et al., 2003). Over-expression of miR-15a significantly increased *Vegfr1* and *Vegfr2* expression (Fig. 5A,B) while these receptors were significantly down-regulated by miR-23b overexpression (Fig. 5A,B). Curiously, overexpression of miR-199a leads to significant *Vefgr2* down-regulation (Fig. 5A,B). Thus these data suggest that miR-15a, miR23b, and miR-199a may also regulate the endocardial EMT repopulation step.

Has2 is responsible for the production of hyaluronic acid (HA), a key component of endocardial cushion cardiac jelly. Importantly, *Has2*-deficient mice have illustrated its importance as a key substrate to facilitate migration of endocardial cells during EMT (Camenisch et al., 2000). Our data revealed no changes in *Has2* expression after miR-15a and miR-23b over-expression, whereas transcript levels significantly decreased after miR-199a over-expression (Fig. 5C). Thus these data suggest that only miR-199a may regulate the remodeling of extracellular matrix.

In summary, our data suggest that miR-15a plays a role as regulator of the delamination/repopulation step while miR-23b and miR-199a broadly and rather similarly affect expression of multiple genes involved in EMT, respectively, being critical to almost all cardiac valve developmental pathways analyzed in this study. Thus, we have focused on the study of miR-23b and miR-199a aiming to dissect whether these microRNAs act at single or multiple levels within the EMT process.

For this purpose, we have performed rescue assays by over-expressing miR-23b or miR-199a, respectively, together with distinct genes functioning at distinct levels in the EMT signaling pathway (Snail, Tbx2, and Bmp2). Specifically, Snail is located in the lower portion of the signaling pathway, whereas Tbx2 and Bmp2 are in the middle and upper portion, respectively. Our results show a partial morphological rescue when overexpressing miR-23b together with Snail while full morphological rescue is observed in all other experimental conditions (Fig. 6A–J).

qRT-PCR analyses of *Snai1* as EMT initiation marker, *Cdh5* as delamination marker, and *Acta2* as mesenchymal differentiation marker revealed that over-expression of *Snail* leads to enhanced increase of *Snai1*, a mild decrease in *Cdh5* expression, while *Acta2* is unaltered, compared to non-transfected controls (Fig. 6K). Tbx2 over-expression down-regulated *Snai1* while *cdh5* and *Acta2* are significantly up-regulated (Fig. 6K). On the other hand, Bmp2 over-expression leads to down-regulation of *Snai1*, while *Cdh5* is unaltered and *Acta2* is up-regulated (Fig. 6K). Overall, these data illustrate the basal molecular changes occurring after EMT Snail, Tbx2, and Bmp2 transfection, respectively, which are essentially in agreement with previous reports. However, in order to understand if over-expression of these EMT genes can rescue miRNA function, data analyzed are based on the comparison to miR-23b and miR-199a transfected explants.

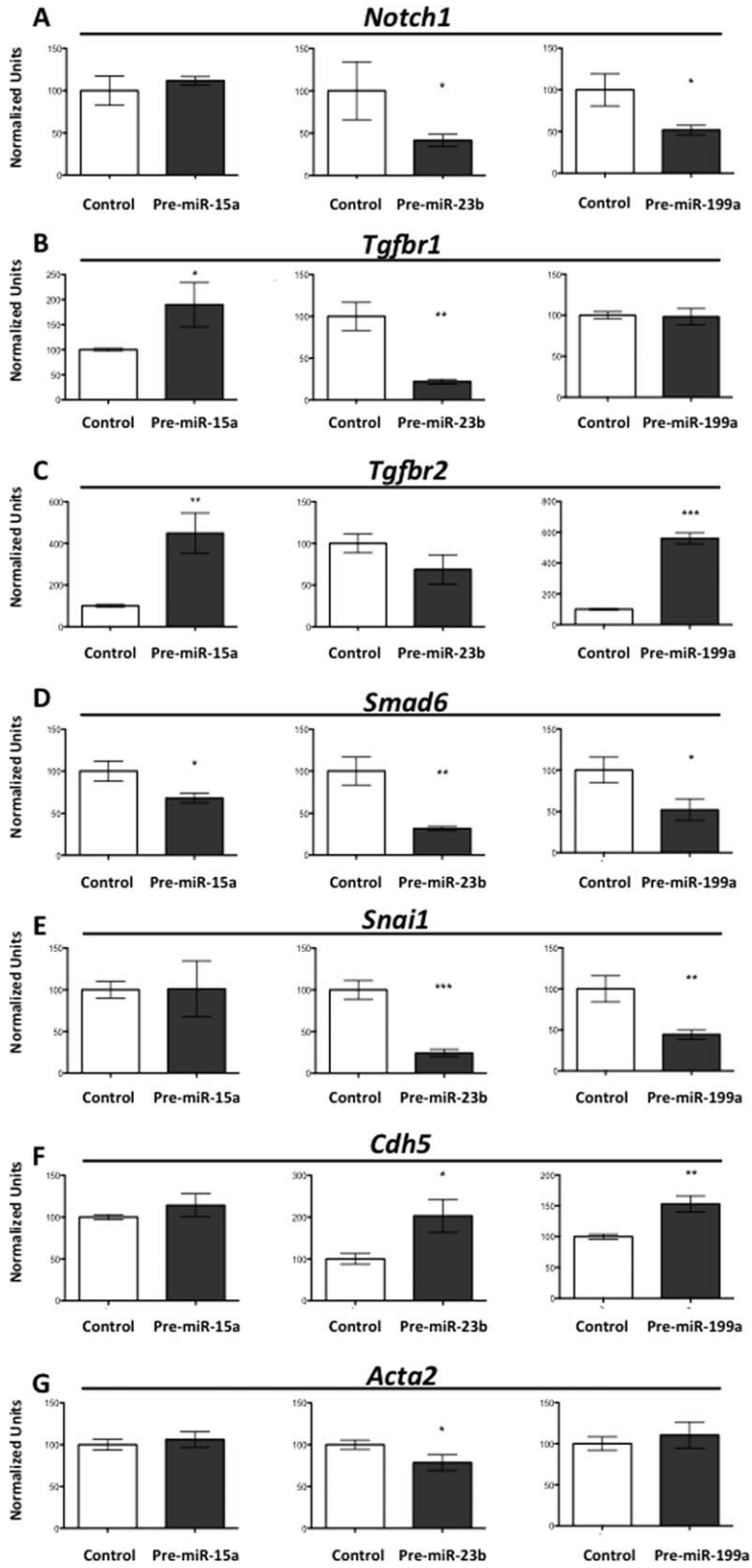

Fig. 4. Expression profiles of EMT signaling pathways genes in AVC explants after pre-miRNAs transfection. **A–G:** qRT-PCR analyses demonstrating different expression levels of distinct genes involved in distinct atrioventricular EMT signaling pathways after pre-miRNAs transfected as compared to controls. As it can be observed, Tgf-beta signaling is impaired after miR-15a over-expression. On the other hand, miR-13b impairs the expression of genes involved in Notch and Tgf-beta signaling as well as *Snai1*, *Chd5,* and *Acta2* expression, in a similar fashion to miR-199a over-expression (with the exception of *Acta2*). Relative levels of expression were normalized using *Gapdh* and *Gusb* as internal controls. * $P < 0.05$, ** $P < 0.01$, *** $P < 0.001$.

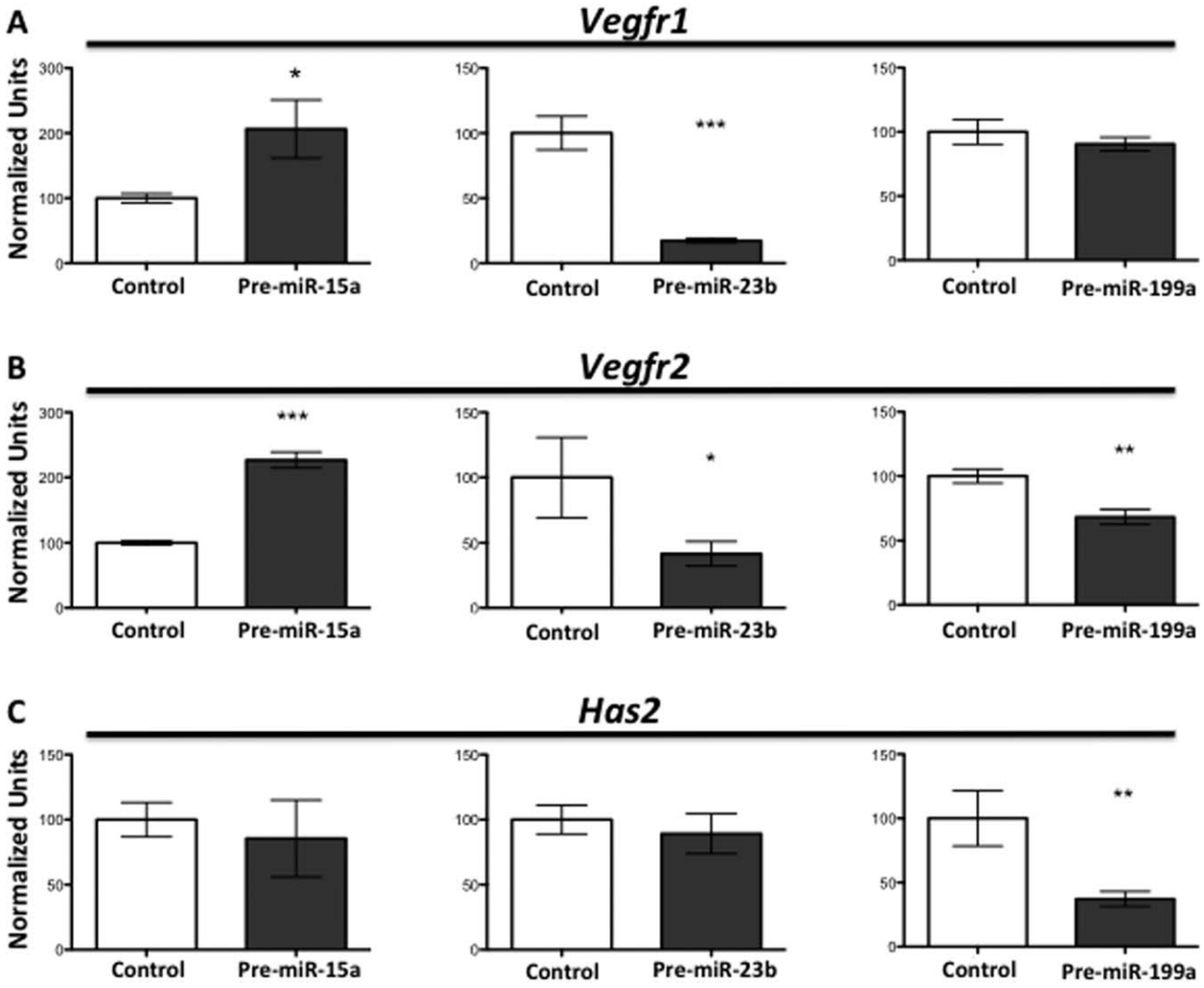

Fig. 5. Expression profiles of EMT signaling pathways genes in AVC explants after pre-miRNAs transfection. **A–C:** qRT-PCR analyses demonstrating different expression levels of distinct genes involved in distinct atrioventricular EMT signaling pathways after pre-miRNAs transfection compared to controls. As it can be noted, genes involved in Vegf signaling are altered after miR-15a, miR-23b, and miR-199a over-expression, respectively. On the other hand, *Has2* expression is only impaired after miR-199a transfection. Relative levels of expression were normalized using *Gapdh* and *Gusb* as internal controls.* $P < 0.05$, ** $P < 0.01$, *** $P < 0.001$.

In this setting, overexpression of miR-23b together with Snail leads to *Cdh5* and *Acta2* down-regulation (Fig. 6L). On the other hand, overexpression of miR-23b and Tbx2 leads to *Cdh5* and *Acta2* up-regulation while no changes were observed for *Snail* (Fig. 6M). Finally, overexpression of miR-23b and Bmp2 results in *Cdh5* down-regulation whereas no changes were observed for *Snail* and *Acta2* (Fig. 6N). Thus these results suggest that in the context of miR-23b overexpression, Snail and Bmp2 may rescue delamination but not mesenchymal differentiation as depicted in Figure 6Q whereas Tbx2 may lead to mesenchymal differentiation without delamination (Fig. 6P) in contrast to the normal EMT process as depicted in Figure 60.qPCR analyses of miR-199a and Snail overexpression lead to up-regulation of *Cdh5* and *Acta2* in AVC explants (Fig. 6L) while overexpression of miR-199a either with Tbx2 or Bmp2, leads in both cases to *Snail*, *Cdh5,* and *Acta2* up-regulation (Fig. 6M,N). Thus, in the context of miR-199a overexpression, Snail, Tbx2, and Bmp2 rescue the mesenchymal differentiation defect but without delamination (Fig. 6P).

Identification of New Genes Modulated by miR-23b and/or miR-199a During Valve Development

Since miR-23b and miR-199a block the EMT process in a rather similar fashion and current knowledge of direct targets for these microRNAs in the EMT context is scarce, we aimed to identify novel putative EMT-related targets and experimentally dissect if those could be modulated after miR-23b and/or miR-199a over-expression in AVC explants. TargetScan predict results in a large number of transcripts for both miR-23b (~800 transcripts) and miR-199 (~400 transcripts), respectively. Importantly, only 66 genes share putative target sites for both miR-23b and miR-199a, respectively. From these 66 genes, we have selected those genes previously described in the literature that play a role in the EMT process in any biological context or within any EMT-related signaling pathway (Bmp, Tgf-beta, Vegf, and/or Notch signaling) or having a cardiac valve expression in E14.5 mouse embryos as revealed using the Genepaint database (www.genepaint.org).

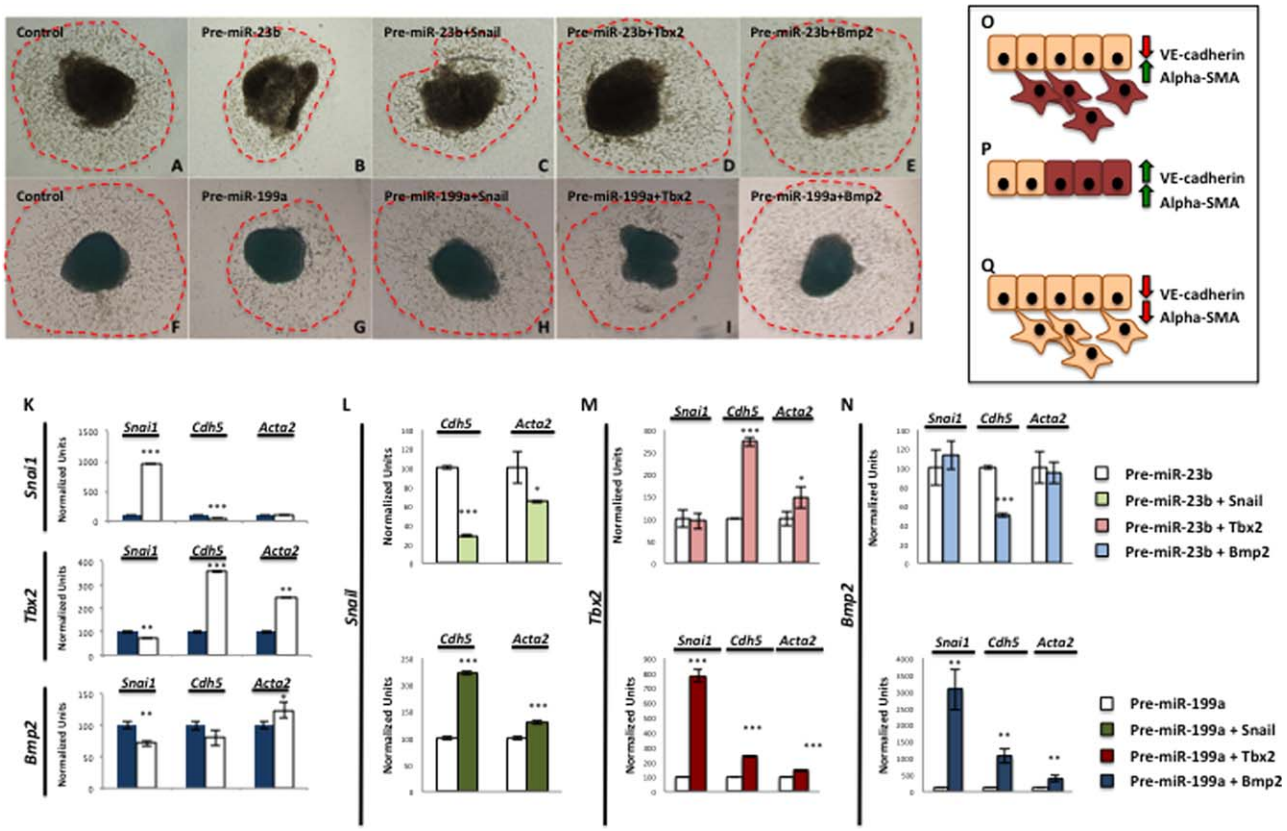

Fig. 6. miR-23b and miR-199a act at distinct levels in the EMT signaling pathways. **A–J:** Inverted microscopy images of AVC explants incubated during 48 hr after co-transfection with Snail, Tbx2, or Bmp2 together miR-23b or miR-199a, respectively. Total morphological rescue is observed for all conditions except for miR-23b+Snail condition. **K:** qRT-PCR analyses of the expression level of distinct EMT markers after transfection with Snail, Tbx2, and Bmp2 expression vectors, respectively, in AVC explants. Observe that after Snail transfection, *Cdh5* is down-regulated while no changes are observed for *Acta2*. Tbx2 and Bmp2 transfection leads to selective down-regulation of *Snail* and up-regulation of *Acta2*, respectively. *Cdh5* is up-regulated after Tbx2 but not Bmp2 transfection. **L–N:** qRT-PCR data showing *Snai1*, *Cdh5,* and *Acta2* expression profiles in AVC explants incubated for 48 hr after co-transfection of Snail, Tbx2, or Bmp2 together miR-23b or miR-199a, respectively. *Snai1* expression is up-regulated when Tbx2 or Bmp2 is co-transfected with miR-199a, respectively. *Cdh5* expression is down-regulated when Snail or Bmp2 is co-transfected with miR-23b, respectively, while in contrast, it is up-regulated in the other conditions. *Acta2* expression is up-regulated in all conditions except when miR-23b is co-transfected with Snail or Bmp2, respectively. **O–Q:** Schematic representation of the distinct morphogenetic models of EMT impairment (O, P) or normal development (Q), based on the expression profiles of *Cdh5* and *Acta2* expression in AVC explants co-transfected with Snail, Tbx2, or Bmp2 together miR-23b or miR-199a, respectively. O depicts the normal condition, in which VE-cadherin is down-regulated, allowing endothelial cells to detach and to acquire a mesenchymal phenotype, as revealed by alpha-SMA expression. P: Mesenchymal differentiation is promoted but cells are unable to detach since VE-cadherin levels are up-regulated. On the contrary, cells are prone to detach but not mesenchymal phenotype is acquired as depicted in Q. Relative levels of expression were normalized using *Gapdh* and *Gusb* as internal controls. * $P < 0.05$, ** $P < 0.01$, *** $P < 0.001$.

A total of 14 candidate genes (*Abca1, Acvr1c, Dcbld2, Erbb4, G3bp2, Gja1, Itgb8, Itpk1, Mapre1, Nfia, Qki, Taok1, Wnk1,* and *Zeb1*) fulfilled those criteria and thus represent putative novel genes involved in AVC EMT process that could be independently modulated by miR-23b and/or miR-199a. All these genes, except *Acvr1c*, display robust and consistent expression in HH17 AVC chicken explants (data not shown).

Experimental EMT in vitro assays were performed as previously described and qRT-PCR analyses demonstrated that most of these novel candidate genes (10/13; ~76%) (*Abca1, Dcbld2, Erbb4, Gja1, Itpk1, Mapre1, Nfia, Qki, Taok1,* and *Zeb1*) were down-regulated after overexpression of both miR-23b and miR-199a in AVC explants (Fig. 7A–M), respectively. Two genes (2/13; ~15%) (*Wnk1* and *Itgb8*) were downregulated only when overexpressed with miR-23b (Fig. 7G, L) while *G3bp2* (1/13; ~8%) was up-regulated after overexpression of both miR-23b and miR-199a, respectively (Fig. 7D). Therefore, we have identified 13 new genes modulated by miR-23b and miR199a that may be involved in the EMT process.

Snail Modulates Multiple EMT miR-23b/miR-199a-Targeted Genes

To obtain further insights into the hierarchical position of these novel EMT miR-23b/miR-199-targeted genes, their expression levels were analyzed after overexpression of Snail, Tbx2, and Bmp2 in AVC explants. Our data demonstrated that overexpression of Bmp2 leads to up-regulation of *Itpk1*, *Mapre1,* and *Nfia*, down-regulation of *Erbb4*, *G3bp2*, *Gja1*, *Qk1,* and *Taok1*, whereas no changes were observed for *Abca1*, *Dcbld2*, *Wnk1,* and *Zeb1* (Fig. 8A). Tbx2 overexpression results in up-regulation of *Dcbld2*, *Itpk1*, *Nfia,* and *Zeb1*, down-regulation of *Erbb4*, *G3bp2*, *Gja1*, *Qk1,* and *Taok1,* whereas no changes were detected for *Abca1*, *Mapre1,* and *Wnk1* (Fig. 8B). Snail overexpression

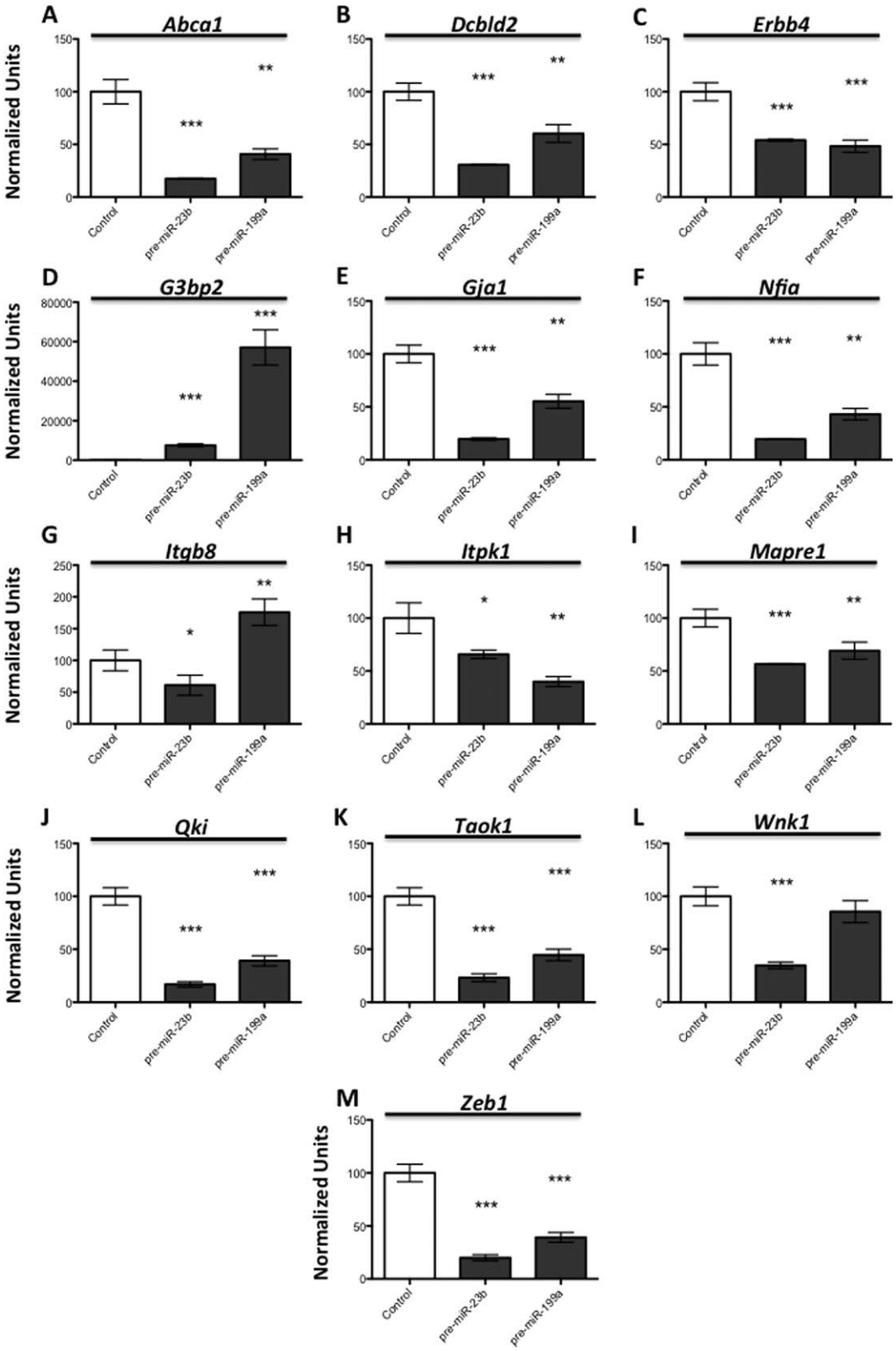

Fig. 7. Expression profile of novel EMT-related genes in AVC explants after pre-miRNAs transfection. **A–M:** qRT-PCR analyses demonstrating differential expression levels of novel EMT-related genes in AVC explants after pre-miRNA transfection as compared to controls (24 hours incubation). Note that all genes display differential expression when either miR-23 and/or miR-199a was transfected in AVC explants compared to controls. Importantly, all novel EMT-related genes, except *G3bp2*, are significantly diminished after pre-miRNA treatment. Relative levels of expression were normalized using *Gapdh* and *Gusb* as internal controls.* $P < 0.05$, ** $P < 0.01$, *** $P < 0.001$.

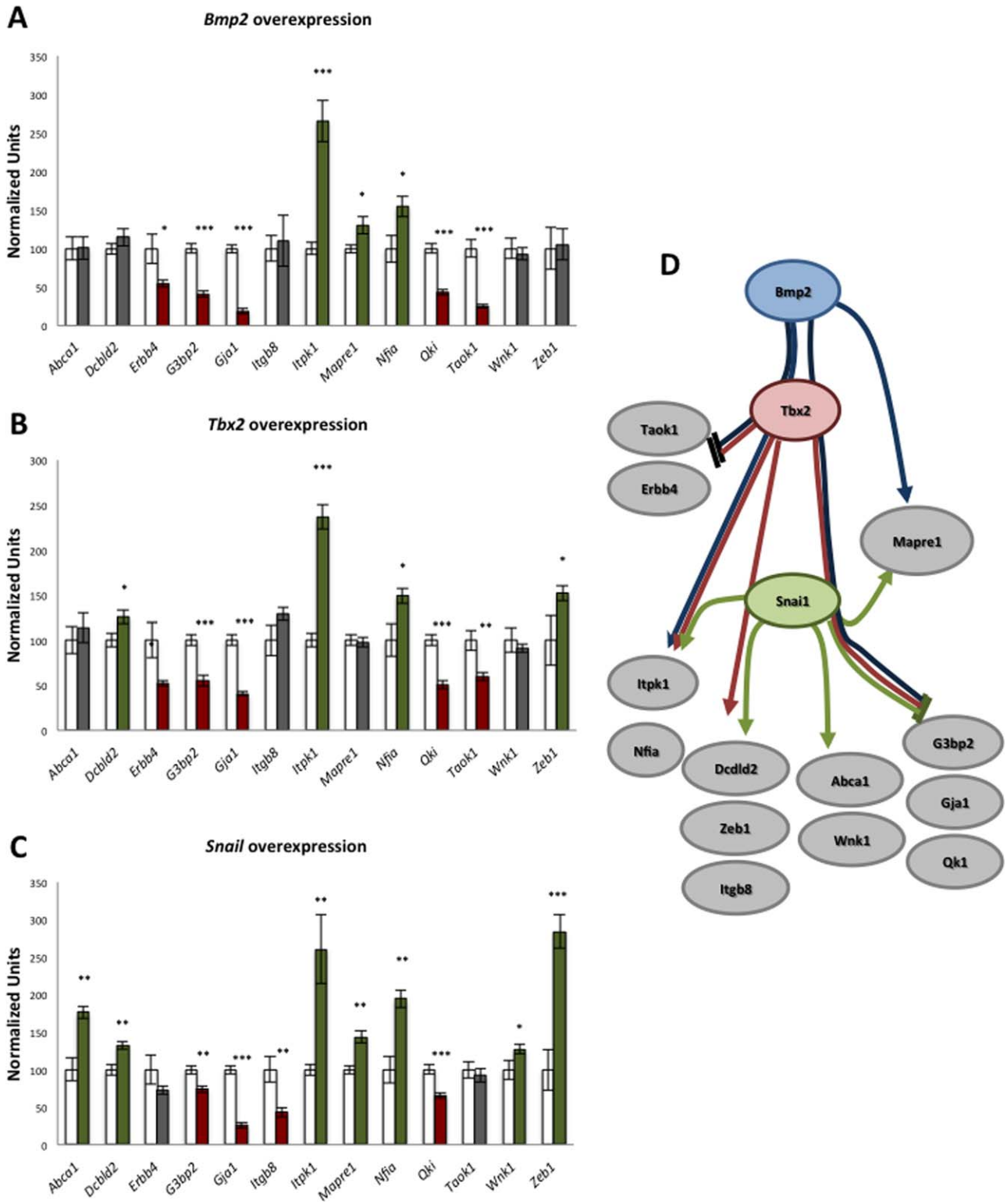

Fig. 8. Expression profile of novel EMT-related genes in AVC explants after Snail, Tbx2, or Bmp2 overexpression. **A–C:** qRT-PCR analyses illustrating the differential expression levels of novel EMT-related genes in AVC explants transfected with Bmp2 (A), Tbx2 (B), and Snail (C), respectively after 48 hr of transfection. Red bars delineate those genes significantly down-regulated whereas green bars delineate those genes significantly up-regulated after corresponding transfection. Grey bars demonstrate no significant differences. It is important to realize that most of these novel EMT-related genes are similarly regulated by Bmp2 and Tbx2, except for *Dcdld2*, *Mapre1,* and *Zeb1*. Interestingly, *Snail* regulates all novel EMT-related genes, except *Erbb4* and *Taok1*. Based on the differentially regulation exerted by transfection with Bmp2, Tbx2, and Snail, respectively, a schematic representation delineating the plausible location of the different genes in the EMT signaling pathway has been drawn on **D**. Relative levels of expression were normalized using *Gapdh* and *Gusb* as internal controls. $^{*}P < 0.05$, $^{**}P < 0.01$, $^{***}P < 0.001$.

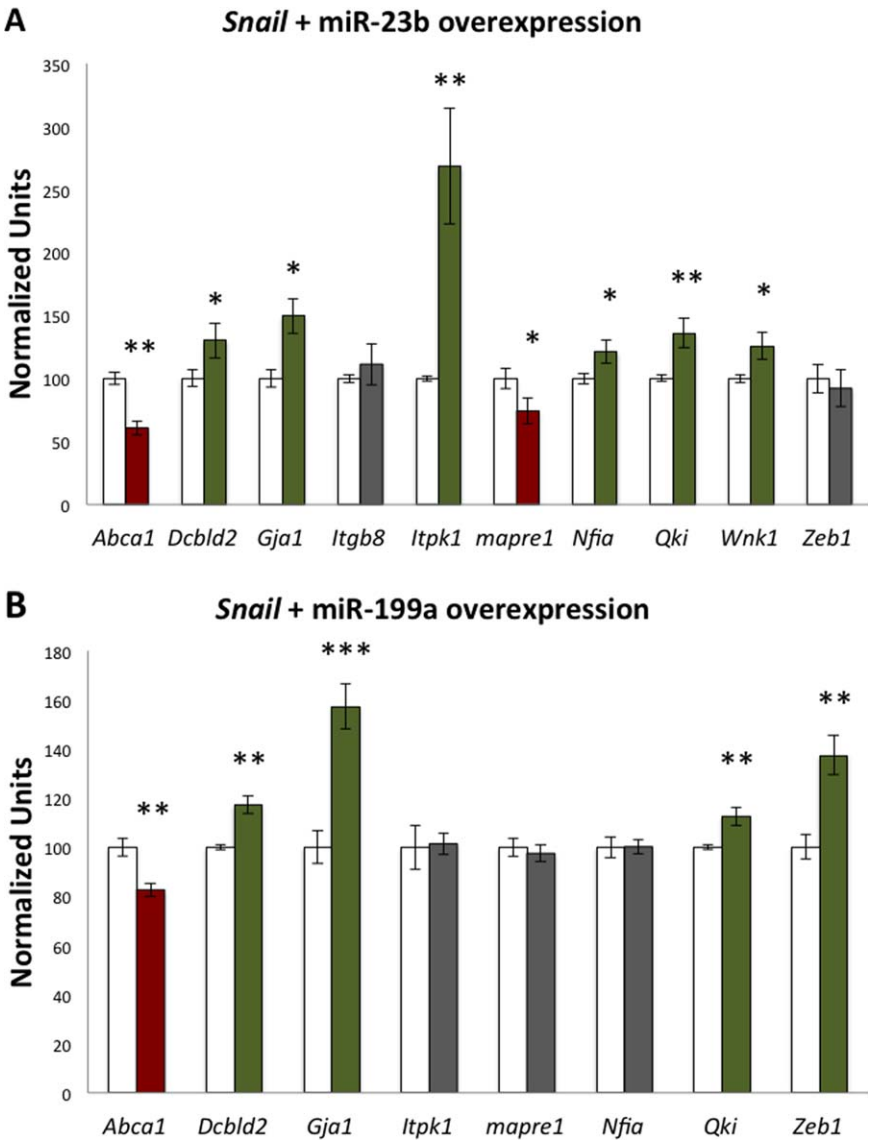

Fig. 9. Expression profile of novel EMT-related genes in AVC explants after overexpression of Snail, Tbx2, or Bmp2 together with miR-23b or miR-199a. **A,B:** qRT-PCR analyses illustrating the differential expression levels of novel EMT-related genes in AVC explants co-transfected with Snail together miR-23b or miR-199a as compared to controls (pre-miRNA transfection alone, respectively). Red bars delineate those genes significantly down-regulated whereas green bars delineate those genes significantly up-regulated after corresponding transfection. Grey bars demonstrate no significant differences. Note that Snail overexpression compensates the effect caused by miR-23b for most of the analyzed novel EMT-related genes (A), whereas it only compensates a subset in the context of miR-199a transfection (B). Relative levels of expression were normalized using *Gapdh* and *Gusb* as internal controls. $^{*}P<0.05$, $^{**}P<0.01$.

leads to up-regulation of *Abca1*, *Dcbld2*, *Itpk1*, *Mapre1*, *Nfia*, *Wnk1,* and *Zeb1* (Fig. 8C) while *G3bp2*, *Gja1*, *Itgb8,* and *Qk1* were down-regulated (Fig. 8C), indicating that these three genes are induced and inhibited, respectively, by Snail. Curiously no changes were observed in *Erbb4* and *Taok1* expression levels suggesting a Snail-independent regulation (Fig. 8C).

Overall these data suggest that *Itpk1* and *Nfia* are induced by Bmp2, Tbx2, and Snail. *Dcbld2* and *Zeb1* are induced by Tbx2 and Snail whereas *Acba1* and *Wnk1* are only induced by Snail. On the other hand, *G3bp2, Gja1,* and *Qk1* are inhibited by all three EMT signaling genes, Bmp2, Tbx2, and Snail, while *Itgb8* is inhibited only by Snail as depicted in Figure 8D. In contrast, *Erbb4* and *Taok1* expression levels were inhibited after Tbx2 and Bmp2 overexpression (Fig. 8D), but independently of Snail overexpression. Finally, *Mapre1* was inhibited after Snail and Bmp2 overexpression (Fig. 8D). Thus, these data suggest that most of the novel EMT miR-23b/miR-199a-targeted genes are regulated by Snail, providing further insights into their putative functional and regulatory role during atrioventricular EMT.

Snail-Mediated Transcriptional Activity Partially Overrules miR-23 and miR-199 Mediated Post-Transcriptional Regulation

To get further insights into the intricate complexity of transcriptional and post-transcriptional regulatory mechanisms governing EMT signaling, we explored whether Snail transcriptional

transactivation is able to compensate for the effect caused by microRNA-mediated post-transcriptional regulation. For this purpose, we performed rescue assays by co-transfecting Snail together with miR-23b and miR-199a in HH17 AVC explants and comparing them with miR-23b transfected explants for genes previously reported to be downstream of Snail (Fig. 9).

Our results show that after co-expression of Snail and miR-23b, six genes (6/10; 60%; *Dcbld2, Gja1, Itpk1, Nfia, Qki,* and *Wnk1*), were significantly up-regulated, two (2/10; 20%; *Abca1* and *Mapre1*) were significantly down-regulated, whereas no significant differences were observed for the expression of *Itgb8* and *Zeb1* (2/10; 20%) as compared to control condition with pre-miR-23b overexpression alone (Fig. 9A). Thus these data suggest that Snail over-expression can compensate for the inactivation mediated by miR-23b in most of the cases (Fig. 9A).

Similarly, co-expression of Snail together miR-199a leads to significant up-regulation of four genes (4/8; 50%; *Dcbld2, Gja1, Qki* and *Zeb1*), significant down-regulation of *Abca1* (1/8; 12.5%), while no significant changes were observed for other three genes (3/8; 37.5%; *Itpk1, Mapre1,* and *Nfia*), Thus these data suggest that Snail over-expression can compensate for the inactivation mediated by miR-199a only in a subset of the analyzed genes (Fig. 9B).

Overall, these results demonstrate that Snail rescues the expression levels of a subset of genes (*Dcbld2*, *Gja1,* and *Qki*) after miR-23b or miR-199a overexpression, but not in all cases, suggesting a large impact of post-transcriptional regulatory mechanisms in EMT signaling.

Discussion

Cell specification and differentiation is governed, in multiple cases, by the onset of discrete gene expression domains during embryonic development (Srivastava and Olson, 2000). In this context, multiple genes have been reported to display regionalized expression patterns during cardiogenesis (Franco et al., 1998). In this study, we provide evidence for the first time that microRNA expression is also regionalized during heart development. qRT-PCR analysis demonstrates a highly dynamic and chamber-enriched differential expression for multiple microRNAs within atrial, ventricular, and atrioventricular canal regions of the developing chicken heart. Such enhanced expression patterns in the atrial or ventricular chambers, respectively, suggest a plausible role for these microRNAs in regulating chamber-specific expression, such as those genes revealing chambered restricted expression, i.e., sarcomere genes (Franco et al., 1998). In accordance with this notion, miR-1 has been reported to inhibit α-myosin heavy chain expression during embryonic stem cell differentiation (Takaya et al., 2009). We have focused our attention on those microRNAs differentially expressed in the AVC. Pre-microRNA over-expression assays have demonstrated that those microRNAs with enhanced expression in the AVC (miR-15a, miR-23b, and miR-199a) are those exerting a more robust EMT inhibition phenotype on overexpression in vitro, whereas over-expression of those microRNAs under-represented in the developing AVC (miR-130a and miR-200a) are unable to block EMT.

miR-15 Has a Discrete Impact on EMT Signaling

miR-15a has been demonstrated to down-regulate several genes involved in EMT, such as, e.g., *Vegf, Bmi-1,* and *AP4,* in multiple cancer types (Peinado et al., 2007; Bhattacharya et al., 2009; Roccaro et al., 2009; Yang et al., 2010; Zhai and Ju, 2011; Guo et al., 2011, 2014; Zheng and Kang, 2013; Shi et al., 2014); however, to date no functional role has been reported for this microRNA during cardiovascular development. In this study, we provided evidence that miR-15 overexpression significantly blocks EMT in chick embryonic AVC explants. Consistent with previous reports, miR-15a modulates Vegf signaling, by increasing expression levels of *Vegfr1* (Flt1) and *Vegfr2* (Kdr). In addition, we demonstrate that Tgf-beta signaling, i.e., *Tgfbr1* and *Tgfbr2*, is also significantly up-regulated. Surprisingly, *Snail*, *Cdh5,* and *Acta2* are not significantly modified, supporting the notion that only a subset of EMT signaling pathways are altered and consistent with the fact that EMT is only partially impaired.

miR-23b Acts at Multiple Levels During EMT Signaling

miR-23b is significantly up-regulated in the AVC region during chicken embryonic development and miR-23b over-expression consistently impaired EMT in embryonic chicken AVC explants. Several previous lines of evidence demonstrated that miR-23b has a pivotal role in EMT signaling by down- and up-regulating *Snai1* and E-cadherin, respectively, in prostate cancer (Majid et al., 2012). Similarly, miR-23b is capable of down-regulating Notch1 expression in dendritic cells (Zheng et al., 2012). In agreement with these reports, we demonstrate herein that miR-23b consistently down-regulates *Notch1* and *Snai1* and up-regulates *Cdh5* during EMT process of chicken embryonic AVC explants. In addition, we also provide novel insights into the regulatory roles of miR-23b in Tgf-beta and Vegf-signaling, since *Tgfbr1*, *Tgfbr2*, *Smad6*, *Vefgr1,* and *Vegfr2* are also significantly down-regulated after miR-23b over-expression. Lagendijk et al. (2011) demonstrated that miR-23 is required to restrict cardiac valve formation by inhibiting *Has-2* in zebrafish embryos. Furthermore, these authors demonstrated that miR-23 inhibited a Tgf-β-induced EMT in mouse endothelial cells (Lagendijk et al., 2011). Whereas our data corroborate previous findings reported by Lagendijk et al. (2011) on the functional role of miR-23 regulating Tgf-beta signaling, we were unable to detect changes on *Has-2* expression after miR-23 over-expression in chicken AVC explants. While further experimental assays will be needed to investigate these functional differences between species, the fact that no predictive miR-23b target binding site (as revealed by Targetscan software: http://www.targetscan.org/) is identified in chicken Has2 gene might underlie such species-specific differences. Taken together, our data demonstrate that miR-23b modulates multiple genes during EMT signaling. Furthermore, our co-transfection assays of Snail, Tbx2, Bmp2, and miR-23b show for the first time that miR-23b acts at multiple levels during EMT signaling.

miR-199 Also Significantly Blocks AVC EMT Signaling at Multiple Steps

Similarly to miR-23b, miR-199 is notably increased in the chicken AVC region during embryonic development and over-expression of miR-199 in AVC explants leads to significant EMT impairment. Little information is available concerning the role of miR-199a during cardiovascular development as well as during EMT in distinct biological contexts, including oncogenesis. Nonetheless, it is important to highlight that a functional role for miR-199 in regulating *E-cadherin* (Hu et al., 2014), *Smad1* (Lin et al.,

2009), *Smad4* (Zhang et al 2012), *Erbb2* and *Erbb3* (He et al., 2012) has been reported in other biological settings. Thus, we provide herein evidences for the first time that miR-199 impairs *Notch1* and Vegf signaling (*Vegfr2*) in chicken AVC explants. In addition, our data further demonstrate that Tgf-beta signaling (*Tgfbr2* and *Smad6*) is modulated by miR-199, having thus a biological impact on the most downstream cascade of AVC EMT signaling, i.e., *Snai1* and *Cdh5* expression. Furthermore, our rescue experiments demonstrate that Bmp2, Tbx2, and Snail overexpression demonstrate that miR-199a acts mainly downstream of Snail in the EMT signaling pathway. However, we cannot exclude the possibility that miR-199 may act upstream of Bmp2 or even upstream Notch1.

Multiple miR-23b/miR-199-Modulated Genes Involved in EMT Signaling

Post-transcriptional regulation by a single microRNA can potentially mediate modulation of hundreds to thousand transcripts (Bartel, 2004). However, deciphering which of the predicted targets is indeed modulated by such microRNA is time and tissue-specific dependent. We have envisioned a simple shortcut to enriched putative miR-23 and/or miR-199 targets in the context of AVC EMT signaling, by selecting predicted targets that shared putative binding sites from both microRNAs, followed by performing a literature-based search for previous involvement on these genes in EMT signaling and/or displaying endocardial cushion expression during embryonic development. Our in silico analysis resulted in the identification of 14 genes meeting the selection criteria, all of which are either deregulated after miR-23b or miR-199 overexpression in AVC explants, and most of them by both microRNAs (12/13;∼92%). Moreover, most of these genes are regulated by Snail (11/13; ∼84%; *Abca1*, *Dcbld2*, *G3bp2*, *Gja1*, *Itgb8*, *Itpk1*, *Mapre1*, *Nfia*, *Qki*, *Wnk1,* and *Zeb1)*, with the exception of *Erbb4* and *Taok1,* which are nonetheless regulated by Tbx2. With the exception of *Gja1* and *Zeb1,* which were previously reported to be regulated by Snail in other biological contexts (Ryszawy et al., 2014; Smit and Peeper, 2011; Cipley et al., 2012), our data demonstrate for the first time that these newly identified genes are regulated by Snail, a critical transcription factor in EMT signaling and modulated by miR-23b and miR-199, thus supporting a critical role of these microRNAs in EMT.

Transcriptional and Post-Transcriptional Regulatory Mechanisms Regulate EMT

Transcriptional as well as post-transcriptional regulatory mechanisms exert control in multiple biological contexts (Bartel, 2004) and as we show here also during EMT signaling in the embryonic AVC. However, it remains rather obscure which of these mechanisms has the more robust impact on EMT signaling. Thus we envisioned a competition assay by over-expressing Snail concomitantly with miR-23 or miR-199, respectively, and assessing expression of distinct Snail-dependent and miRNA-dependent genes. Our result demonstrated that in both microRNA overexpression contexts (miR-23b and miR-199, respectively), Snail was able to compensate the effect caused by these microRNAs in approximately half of these genes (miR-23b, 6/10=60%; *Dcbld2*, *Gja1*, *Itpk1*, *Nfia*, *Qki,* and *Wnk1*; miR-199, 5/9= 65%; *Dcbld2*, *G3bp2*, *Gja1*, *Qki*, and *Zeb1*). Therefore, these results seem to indicate transcriptional and post-transcriptional regulation is equally robust in controlling expression of EMT-downstream genes, and support the conclusion that both mechanisms play pivotal roles during EMT in chicken embryonic AVC explants.

In summary, our data demonstrate that miR-15a, miR-23b, and miR-199a block significantly the EMT process using HH17 embryonic chicken AVC explant culture by modulating distinct EMT steps. Furthermore, our analyses identified novel genes modulated by miR-23b and/or miR-199a in the AVC, most of which are also regulated by Snail, Tbx2, and Bmp2, either increasing or inhibiting their expression. Overall these data suggest that these genes would be involved in the atrioventricular EMT, yet additional experiments are required to validate this claim.

Experimental Methods

Tissue Samples

Fertilized eggs from white Leghorn chickens (Granja Santa Isabel, Córdoba, Spain) were incubated at 37.5°C and 50% humidity for 2–7 days. Embryos were harvested at different developmental stages (HH13, HH17, HH20, HH27, and HH31) and classified according to Hamburger and Hamilton (1951). Embryos were removed from the egg by cutting the blastocyst margin with iridectomy scissors and placing them into Earle's balanced salt solution (EBSS) (Gibco).

For qPCR analyses, hearts were isolated and then atrial, ventricular, and atrioventricular canal regions were dissected out, pooled (n=10), and stored at -80°C until used. For in vitro explants cultures, chicken HH17 atrioventricular canal (AVC) were dissected in Earle's balanced salt solution (EBSS) (Gibco) and cut in two halves to expose the inner endocardial surface to the collagen gels as previously described (Bernanke and Markwald, 1982), in such a way that the endocardium is in direct contact with the gel surface to facilitate endothelium cell outgrowth.

Transfection of AVC Explants (microRNA precursors and plasmids)

AVC explants were cultured on collagen gels and incubated for 6 hr at 37°C in a cell culture incubator before pre-miRNAs (microRNA precursors) or plasmid transfection, respectively. Pre-miRNAs transfections were carried out with Lipofectamine 2000 (Invitrogen), following the manufacturer's guidelines. Briefly, 85 ρM of pre-miRNA were applied to the explants (3–5 explants per well) for 24–48 hr. Plasmids transfections were also carried out using Lipofectamine 2000 (Invitrogen) as described above. Briefly, 500 ng of pcDNA3-Snail (kindly provided by Dr. M. Ángeles Nieto, Madrid, Spain), pcDNA3-Tbx2 (kindly provided by Dr. Vincent Christoffels, Amsterdam, The Netherlands) or pCAGs-Bmp2 alone or premixed with the corresponding pre-miRNA and Lipofectamine 2000 were applied to the AVC explants. After 24 hr (pre-miRNAs) and 48 hr (plasmids) of incubation, explants were either processed for qRT-PCR or immunohistochemical (IHC) analyses. Negative controls, i.e., AVC explants treated only with Lipofectamine were run in parallel. Similarly, positive EMT blockage controls, i.e., AVC explants treated with high glucose (20 mM), were also assayed. To perform IHC analyses, the myocardium layer was removed after explant culture and the remaining tissues were fixed with 1% PFA for 2 hr at 4°C, rinsed for three times in PBS during 10 min, and stored in PBS at 4°C until further processed. For qRT-PCR analyses,

TABLE 1. Bonet et al.

Gene	Specie	Oligo	Sequences
Abca1 (NM_204145.2)	*Gallus gallus*	GgAbca1 F	TACTGTCCGCAGTTTGATGC
		GgAbca1 R	AATGAGGGCTATTGCTGTGG
Actg2 (NM_205172.1)	*Gallus gallus*	GgActg2 F	GGCTCAAAGCAAGAGAGGAA
		GgActg2 R	ATTGGCTTTGGGATTCAGTG
Acvr1c (XM_422170.3)	*Gallus gallus*	GgAcvr1c F	ACATGGCTCCCGAGATACTG
		GgAcvr1c R	GGAGCTTCTGCTCACAAACC
Cdh5 (NM_204227.1)	*Gallus gallus*	GgCdh5 F	ACGCACAAGTTCACGTCATT
		GgCdh5 R	TGTGAAGAAACCTCCAGGTGA
DcbId2 (NM_001025954.1)	*Gallus gallus*	GgDcbId2 F	ACGCTACAGCAGCAGTGAAA
		GgDcbId2 R	AGGCAGTGGTTCAGCATAGG
Erbb4 (NM_001030365.1)	*Gallus gallus*	GgErbb4 F	CGATGAGGAAGACCTGGAAG
		GgErbb4 R	CAGGAGCTCTGTACGGCATC
FIt1 (NM_204252.1)	*Gallus gallus*	GgVegfr1 (FIt) F	GCAGCCAGAAACATCCTTTT
		GgVegfr1 (FIt) R	ACACATCGCTTTTGGTGTTG
G3bp2 (XM_420536.3)	*Gallus gallus*	GgG3bp2 F	CGAATAATCCGCTACCCAGA
		GgG3bp2 R	TCTGGACTGGCTCAGAATCA
Gapdh (NM_204305.1)	*Gallus gallus*	GgGapdh F	TGTCCTCTCTGGCAAAGTCC
		GgGapdh R	TGCCCATTGATCACAAGTTT
Gja1 (NM_204586.2)	*Gallus gallus*	GgGJja1 F	TGCTCTTCCGTTTTCCCTTA
		GgGja1 R	CCAATAGCAGGATTCGGAAA
Gusb (NM_001039316.2)	*Gallus gallus*	GgGusb F	CGTACCAGCCACTACCCCTA
		GgGusb R	TTATCCCTGCGGATCAGTTC
Has2 (NM_204806.1)	*Gallus gallus*	GgHas2 F	CAGAAATGGGGTGGAAAAAG
		GgHas2 R	CCTCCAACCATTGGATCTTC
Itgb8 (XM_003640686.1)	*Gallus gallus*	GgItgb8 F	TTGTGTTCAGTGCCACCATT
		GgItgb8 R	CAACAAGCAACCCAATCAGA
Itpk1 (NM_001012588.1)	*Gallus gallus*	GgItpk1 F	TGATGTCATCCGGGAAATCT
		GgItpk1 R	CAGCAGCTATGTGGTTCAGG
Kdr (NM_001004368.1)	*Gallus gallus*	GgVegfr2 (KDR) F	CAGGCATGGTCTTCTGTGAA
		GgVegfr2 (KDR) R	AATCAATTCCCACGTTCAGC
Mapre1 (NM_001030860.1)	*Gallus gallus*	GgMapre1 F	AAAAAGGCTGCAGGAGATGA
		GgMapre1 R	GGCGTAAAGGATTTCCACAA
Nfia (NM_205273.1)	*Gallus gallus*	GgNfia F	CTACTCGACACCCAGCACCT
		GgNfia R	CTGCTGCTTCCGTGTTACAG
Notch1 (XM_415420.3)	*Gallus gallus*	GgNotch1 F	GAAGAACGGTGCCAATAAGG
		GgGapdh R	TGCCCATTGATCACAAGTTT
Qki (NM_204310.2)	*Gallus gallus*	GgQki F	GGACCCGAAGCTGGTTTAAT
		GgQki R	GTCTGCGGTCACAATCCTTT
Smad6 (NM_204248.1)	*Gallus gallus*	GgSmad6 F	CGCACTGCTAACGCTGAG
		GgSmad6 R	CGTGACGTTGGGTGAGTTC
Taok1 (XM_415829.3)	*Gallus gallus*	GgTaok1 F	TGCGTGATCTTGAACAGAGG
		GgTaok1 R	CCTCGGGGGAGAGATTAGAA
Tgfβr1 (NM_204246.1)	*Gallus gallus*	GgTgfβR1 F	GGAAATTGCTCGTCGATGTT
		GgTgfβR1 R	TCACAGCTCTGCCATCTGTT
TgfβrII (NM_205428.1)	*Gallus gallus*	GgTgfβRII F	CGAGCAACTGCAACATCACT
		GgTgfβRII R	GCTCTGAGCTGGAGTCATCC
Wnk1 (XM_001235130.2)	*Gallus gallus*	GgWnk1 F	CCGAAAAGGGACTTTCACAG
		GgWnk1 R	TAGCACCCAGGGAAGATGTC
Zeb1 (NM_205131.1)	*Gallus gallus*	GgZeb1 F	GCTGCCAATAAGCAAACCAT
		GgZeb1 R	TGGGGGTGTTGAATCAGAAT

AVC explants were carefully dissected, including part of the underlying collagen gel, placed into 1.5-mL microcentrifuge tubes, and stored at -80°C until used.

RNA Isolation and qRT-PCR (mRNA and microRNAs)

All qRT-PCR experiments followed MIQE guidelines (Bustin et al., 2009). RNA was extracted and purified by using Trizol reactive (Invitrogen) according to the manufacturer's instructions. For mRNA expression measurements, 1 μg of total RNA was used for retro-transcription with Maxima First Strand cDNA Synthesis Kit for RT-qPCR (Thermo Scientific). Real time PCR experiments were performed with 1 μL of cDNA, SsoFast EvaGreen mix and corresponding primer sets as described on Table 1. For microRNA expression analyses, 20 ng of total RNA was used for retro-transcription with Universal cDNA Synthesis Kit II (Exiqon) and

the resulting cDNA was diluted 1/80. Real time PCR experiments were performed with 1 μL of diluted cDNA, ExiLENT SYBR® Green master mix (Exiqon) and corresponding primer sets described on Table 1. All qPCRs were performed using a CFX384TM thermocycler (Bio-Rad) following the manufacturer's recommendations. The relative level of expression of each gene was calculated as described by Livak and Schmittgen (2001) using *Gapdh* and *Gusb* as internal control for mRNA expression analyses and *5S* and *6U* for microRNA expression analyses, respectively. Each PCR reaction was carried out in triplicate and repeated in at least three distinct biological samples to obtain representative means.

Immunofluorescence Analysis by Confocal Scanning Laser Microscopy

Control and transfected AVC explants were collected after 24 hr of incubation, rinsed in PBS for 10 min at room temperature, and fixed with 1% PFA for 2 hr at 4°C. After fixation, the explants were rinsed three times (10 min each) in PBS at room temperature. The explants were then permeabilized with 1% Triton X-100 in PBS for 30 min at room temperature. To block nonspecific binding sites, PBS containing 5% goat serum and 1% bovine serum albumin (Sigma) was applied to the explants overnight at 4°C. As primary antibody, a monoclonal anti-mouse anti-α-SMA (Sigma) was used, diluted (1:200) in PBS, and applied to the explants overnight at 4°C. Subsequently, AVC explants were rinsed three times (for 1 hr each) in PBS to remove excess primary antibody and incubated overnight at 4°C with Alexa-Fluor 546 anti-mouse (1:100; Invitrogen) as secondary antibody. After incubation with the secondary antibody, the explants were rinsed as described above. Finally, AVC explants were incubated with DAPI (1:1,000; Sigma) for 7 min at room temperature and rinsed three times in PBS for 5 min each. The explants were stored in PBS in darkness at 4°C until analyzed using a Leica TCS SP5 II confocal scanning laser microscope. The ratio of αSMA-positive cells/total DAPI-positive cells was calculated in all Z-stacks. Mean average of all Z-stacks was calculated for each experimental and control condition as a proxy to determine the percentage of cells undergoing EMT.

LNA In Situ Hybridization

In situ hybridization was performed in chicken embryos ranging from HH8 to HH20 using double DIG-labeled LNA antisense probes (Exiqon) as previously described (Darnell et al., 2006).

Statistical Analyses

For statistical analyses of datasets, unpaired Student's *t*-tests were used. Significance levels or *P* values are stated in each corresponding figure legend. $P < 0.05$ was considered statistically significant.

Acknowledgments

This work is partially supported by grants-in-aid from the Junta de Andalucía Regional Council to D.F. (CTS-1614) and to A.A. (CTS-03878). This work is partially supported by grants-in-aid from the Junta de Extremadura Regional Council to V.G.M. We thank Dr. Robert Kelly (IBDM, Aix-Marseille University) for a critical reading of the manuscript.

References

American Heart Association. 2004 Heart Disease and Stroke Statistics. http://www.americanheart.org.
Armstrong EJ, Bischoff J. 2004. Heart valve development:endothelial cell signaling and differentiation. Circ Res 95:459–470.
Bartel DP. 2004. MicroRNAs: genomics, biogenesis, mechanism, and function. Cell 116:281–297.
Bernake DH, Markwald RR. 1982. Migratory behavior of cardiac cushion tissue cells in a collagen-lattice culture system. Dev Biol 91:235–245.
Bernhart SH, Tafer H, Mückstein U, Flamm C, Stadler PF, Hofacker IL. 2006. Partition function and base pairing probabilities of RNA heterodimers. Algorithms Mol Biol 16:3–13.
Bhattacharya R, Nicoloso M, Arvizo R, Wang E, Cortez A, Rossi S, Calin GA, Mukherjee P. 2009. MiR-15a and MiR-16 control Bmi-1 expression in ovarian cáncer. Cancer Res 69:9090–9095.
Bolender DL, Markwald RR. 1979. Epithelial-mesenchymal transformation in chick atrioventricular cushion morphogenesis. Scan Electron Microsc 3:313–321.
Bouyssou JM, Manier S, Huynh D, Issa S, Roccaro AM, Ghobrial IM. 2014. Regulation of microRNAs in cancer metastasis. Biochim Biophys Acta 1985:255–265.
Bustin SA, Benes V, Garson JA, Hellemans J, Huggett J, Kubista M, Mueller R, Nolan T, Pfaffl MW, Shipley GL, Vandesompele J, Wittwer CT. 2009. The MIQE guidelines: minimum information for publication of quantitative real-time PCR experiments, Clin Chem 55:611–622.
Camenisch TD, Spicer AP, Brehm-Gibson T, Biesterfeldt J, Augustine ML, Calabro A, Kubalak S, Klewer SE, McDonald JA. 2000. Disruption of hyaluronan synthase-2 abrogates normal cardiac morphogenesis and hyaluronan mediated transformation of epithelium to mesenchyme. J Clin Invest 106:349–360.
Camenisch TD, Spicer AP, Brehm-Gibson T, Biesterfeldt J, Augustine ML, Calabro A, Jr., Kubalak S, Klewer SE, McDonald JA. 2004. Disruption of hyaluronan synthase-2 abrogates normal cardiac morphogenesis and hyaluronan-mediated transformation of epithelium to mesenchyme. J Clin Invest 106:349–360.
Canfrán-Duque A, Ramírez CM, Goedeke L, Lin CS, Fernández-Hernando C. 2014. microRNAs and HDL life cycle. Cardiovasc Res 103:414–422.
Chinchilla A, Lozano E, Daimi H, Esteban FJ, Crist C, Aranega AE, Franco D. 2011. MicroRNA profiling during mouse ventricular maturation: a role for miR- 27 modulating Mef2c expression. Cardiovasc Res 89:98–108.
Cipley B, Riley P 4th, Pifer PM, Widmeyer J, Addison JB, Ivanov AV, Denvir J, Frish SM. 2012. Suppression of the Epithelial–Mesenchymal Transition by Grainyhead-like-2. Cancer Res 72:2440–2453.
Darnell DK, Kaur S, Stanislaw S, Konieczka JH, Yatskievych TA, Antin PB. 2006. MicroRNA expression during chick embryo development. Dev Dyn 235: 3156–3165.
Díaz-Lopez A, Moreno-Bueno G, Cano A. 2014. Role of microRNA in epithelial to mesenchymal transition and metastasis and clinical perspectives. Cancer Manag Res 6:205–216.
Doench JG, Sharp PA. 2004. Specificity of microRNA target selection in translational repression. Genes Dev 18:504–511.
Dor Y, Camenisch TD, Itin A, Fishman GI, McDonald JA, Carmeliet P, Keshet E. 2001. A novel role for VEGF in endocardial cushion formation and its potential contribution to congenital heart defects. Development 128:1531–1538.
Drake CJ, Jacobson AG. 1988. A survey by scanning electron microscopy of the extracellular matrix and endothelial components of the primordial chick heart. Anat Rec 222:391–400.
Enciso JM, Gratzinger D, Camenish TD, Canosa S, Pinter E and Madri JA. 2003. Elevated glucose inhibits VEGF-A-mediated endocardial cushion formation: modulation by PECAM-1 and MMP-2. J Cell Biol 160:605–615.
Feng X, Wang Z, Fillmore R, Xi Y. 2014. MiR-200, a new star miRNA in human cancer. Cancer Lett 344:166–173.
Franco D, Lamers WH, Moorman AF. 1998. Patterns of expression in the developing myocardium: towards a morphologically integrated transcriptional model. Cardiovasc Res 38:25–53.
Gaussin V, Van de Putte T, Mishina Y, Hanks MC, Zwijsen A, Huyle- broeck D, Behringer RR, Schneider MD. 2002.

Endocardial cushion and myo- cardial defects after cardiac myocyte-specific conditional deletion of the bone morphogenetic protein receptor ALK3. PNAS 99:2878–2883.
Guo BH, Feng Y, Zhang R, Xu LH, Li MZ, Kung HF, Song LB, Zeng MS. 2011. Bmi-1 promotes invasion and metastasis, and its elevated expression is correlated with an advanced stage of breast cancer. Mol Cancer 10:10.
Guo S, Xu X,Tang Y,Zhang C,Li J,Ouyang Y,Ju J,Bie P,Wang H. 2014. miR-15a inhibits cell proliferation and epithelial to mesenchymal transition in pancreatic ductal adenocarcinoma by down-regulating Bmi-1 expression. Cancer Lett 344:40–46.
Hata A, Lagna G, Massague J, Hemmati-Brivanlou A. 1998. Smad6 inhibits BMP/Smad1 signaling by specifically competing with the Smad4 tumor suppressor. Genes Dev 12:186–197.
Hay ED. 2005. The mesenchymal cell, its role in the embryo, and the remarkable signaling mechanisms that create it. Dev Dyn 233:706–720.
He J, Xu Q, Jing Y, Agani F, Qian X, Carpenter R, Li Q, Wang XR, Peiper SS, Lu Z, Liu LZ, Jiang BH. 2012. Reactive oxygen species regulate ERBB2 and ERBB3 expression via miR-199a/125b and DNA methylation. EMBO Rep 13:1116–1122.
Hinton Jr RB, Lincoln J, Deutsch GH, Osinska H, Manning PB, Benson DW, Yutzey KE. 2006. Extracellular matrix remodeling and organization in developing and disease aortic valves. Circ Res 98:1431–1438.
Hinton JR Rb, Alfieri CM, Witt SA, Glascock BJ, Khoury PR, Benson DW, Yutzey KE. 2008. Mouse heart valve structure and function: echocardiographic and morphometric analyses from the fetus through the aged adult. Am J Physiol Heart Circ Physiol 294:2480–2488.
Hinton RB, Yutzey KE. 2011. Heart valve structure and function in development and disease. Annu Rev Physiol 73:29–46.
Hu Y, Liu J, Jiang B, Chen J, Fu Z, Bai F, Jiang J, Tang Z. 2014. MiR-199a-5p loss up-regulated DDR1 aggravated colorectal cancer by activating epithelial-to-mesenchymal transition related signaling. Dig Dis Sci 59:2163–2172.
Johnson EN, Lee YM, Sander TL, Rabkin E, Schoen FJ, Kaushal S, Bischoff J. 2003. NFATc1 mediates vascular endothelial growth factor-induced proliferation of human pulmonary valve endothelial cells. J Biol Chem 278:1686–1692.
Kim RY, Robertson EJ, Solloway MJ. 2001. Bmp6 and Bmp7 are required for cushion formation and septation in the developing mouse heart. Dev Biol. 235:449–466.
Kolpa HJ, Peal DS, Lynch SN, Giocas AC, Ghatak S, Misra S, Norris RA, Macrae CA, Markwald RR, Ellinor P, Bischoff J, Milan DJ. 2013. miR-21 represses Pdcd4 during cardiac valvulogenesis. Development 140:2172–2180.
Lagendijk AK, Goumans MJ Burkhard SB, Bakkers J. 2011. MicroRNA-23 restricts cardiac valve formation by inhibiting Has2 and extracellular hyaluronic acid production. Circ Res 109:649–657.
Lamouille S, Subramanyam D, Blelloch R, Derynck R. 2013. Regulation of epithelial-mesenchymal and mesenchymal-epithelial transitions by microRNAs. Curr Opin Cell Biol 25:200–207.
Lin EA, Kong L, Bai XH, Luan Y, Liu CJ. 2009. MiR-199a, a bone morphogenic protein 2-responsive microrna, regulates chondrogenesis via direct targeting to smad1. J Biol Chem 284:11326–11335.
Linask KK, Lash JW. 1993. Early heart development: dynamics of endocardial cell sorting suggests a common origin with cardiomyocytes. Dev Dyn 195:62–69.
Lincoln J, Yutzey KE. 2011. Molecular and developmental mechanisms of congenital heart valve disease. Birth Defects Res A Clin Mol Teratol 91:526–534.
Lincoln J, Alfieri CM, Yutzey KE. 2004. Development of heart valve leaflets and supporting apparatus in chicken and mouse embryos. Dev Dyn 30:239–250.
Livak KJ, Schmittgen TD. 2001. Analysis of relative gene expression data using real-time quantitative PCR and the 2(-Delta Delta C(T)) Method 25:402–408.
Majid S, Dar AA, Saini S, Arora S, Shahryari V, Zaman MS, Chang I, Yamamura S, Tanaka Y, Deng G, Dahiya R. 2012. MiR-23b represses proto-oncogene Src kinase and functions as methylation-silenced tumor suppressor with diagnostic and prognostic significance in prostate cáncer. Cancer Res 72:6435–6446.
Markwald RR, Fitzharris TP, Smith WN. 1975. Structural analysis of endocardial cytodifferentiation. Dev Biol 42:160–180.
Markwald RR, Fitzharris TP, Manasek FJ. 1977. Structural development of endocardial cushions. Am J Anat 148:85–119.
Markwald RR, Norris RA, Moreno-Rodriguez R, Levine RA. 2011. Developmental basis of adult cardiovascular diseases: valvular heart diseases. Ann N Y Acad Sci 1188:177–183.
Miquerol L, Langille BL, Nagy A. 2000. Embryonic development is disrupted by modest increases in vascular endothelial growth factor gene expression. Development 127:3941–3946.
Nakajima Y, Yamagishi T, Hokari S, Nakamura H. 2000. Mechanisms involved in valvuloseptal endocardial cushion formation in early cardiogenesis: roles of transforming growth factor (TGF)-β and bone morphogenetic protein (BMP). Anat Rec 258:119–127.
Peinado H, Olmeda D, Cano A. 2007. Snail, Zeb and bHLH factors in tumour progression: an alliance against the epithelial phenotype? Nat Rev Cancer 7:415–428.
Roccaro AM, Sacco A, Thompson B, Leleu X, Azab AK, Azab F, Runnels J, Jia X, Ngo HT, Melhem MR, Lin CP, Ribatti D, Rollins BJ, Witzig TE, Anderson KC, Ghobrial IM. 2009. MicroRNAs 15a and 16 regulate tumor prolif- eration in multiple myeloma. Blood 113:6669–6680.
Romano LA, Runyan RB. 2000. Slug is an essential target of TGFβ2 signaling in the developing chicken heart. Dev Biol 223:91–102.
Ryszawy D, Sarna M, Rak M, Szpak K, Kedracka-Krok S, Michalik M, Siedlar M, Zuba-Surma E, Burda K, Korohoda W, Madeja Z, Czyz J. 2014. Functional links between Snail-1 and Cx43 account for the recruitment of Cx43-positive cells into the invasive front of prostate cancer. Carcinogenesis 35:1920–1930.
Scanlon CS, Van Tubergen EA, Inglehart RC, D'Silva Nj. 2013. Biomarkers of epithelial-mesenchymal transition in squamous cell carcinoma. J Dent Res 92:114–121.
Shi L, Jackstadt R, Siemens H, Li H, Kirchner T and Hermeking H. 2014. p53- induced miR-15a/16-1 and AP4 form a double-negative feedback loop to regulate epithelial–mesenchymal transition and metastasis in colorectal cancer. Cancer Res 70:532–542.
Smit MA, Peeper DS. 2011. Zeb1 is required for TrkB-induced epithelial-mesenchymal transition, anoikis resistance and metastasis. Oncogene 30:3735–3744.
Srivastava D, Olson EN. 2000. A genetic blueprint for cardiac development. Nature 407:221–226.
Sugi Y, Yamamura H, Okagawa H, Markwald RR. 2004. Bone morphogenetic protein-2 can mediate myocardial regulation of atrioventricular cushion mesenchymal cell formation in mice. Dev Biol 269:505–518.
Synnergren J, Améen C, Lindahl A, Olsson B, Sartipy P. 2011. Expression of microRNAs and their target mRNAs in human stem cell-derived cardiomyocyte clusters and in heart tissue. Physiol Genomics 43:581–594.
Takaya T, Ono K, Kawamura T, Takanabe R, Kaichi S, Morimoto T, Wada H, Kita T, Shimatsu A, Hasegawa K. 2009. MicroRNA-1 and MicroRNA-133 in spontaneous myocardial differentiation of mouse embryonic stem cells. Circ J 73:1492–1497.
Thiery JP, Sleeman JP. 2006. Complex networks orchestrate epithelial- mesenchymal transitions. Nat Rev Mol Cell Biol 7:131–142.
Timmerman LA, Grego-Bessa J, Raya A, Bertran E, Perez-Pomares JM, Diez J, Aranda S, Palomo S, McCormick F, Izpisua-Belmonte JC, de la Pompa JL. 2004. Notch promotes epithelial-mesenchymal transition during cardiac development and oncogenic transformation. Genes Dev 18:99–115.
Vacchi-Suzzi C, Hahne F, Scheubel P, Marcellin M, Dubost V, Westphal M, Boeglen C, Büchmann-Møller S, Cheung MS, Cordier A, De Benedetto C, Deurinck M, Frei M, Moulin P, Oakeley E, Grenet O, Grevot A, Stull R, Theil D, Moggs JG, Marrer E, Couttet P. 2013. Heart structure-specific transcriptomic atlas reveals conserved microRNA-mRNA interactions. PLoS One 8:e52442.
Virágh S, Szabó E, Challice CE. 1989. Formation of the primitive myo- and endocardial tubes in the chicken embryo. J Mol Cell Cardiol 21:123–137.
Westin J, Lardelli M. 1997. Three novel Notch genes in zebrafish: implications for vertebrate Notch gene evolution and function. Dev Genes Evol 207:51–63.

Wirrig EE, Yutzey KE. 2011. Transcriptional regulation of heart valve development and disease. Cardiovasc Pathol 20:162–167.
Yamagishi T, Nakajima Y, Miyazono K, Nakamura H. 1999. Bone morphogenetic protein-2 acts synergistically with transforming growth factor-3 during endothelial-mesenchymal transformation in the developing chick heart. J Cell Physiol 180:35–45.
Yang GF, He WP, Cai MY, He LR, Luo JH, Deng HX, Guan XY, Zeng MS, Zeng YX, Xie D. 2010. Intensive expression of Bmi-1 is a new independent predictor of poor outcome in patients with ovarian carcinoma. BMC Cancer 10:133.
Zhai H, Ju J. 2011. Implications of microRNAs in colorectal cancer development, diagnosis, prognosis, and therapeutics. Front Genet 2:78.
Zhang Y, Fan KJ, Sun Q, Chen AZ, Shen WL, Zhao ZH, Zheng XF, Yang X. 2012. Functional screening for miRNAs targeting Smad4 identified miR-199a as a negative regulator of TGF-β signalling pathway. Nucleic Acids Res 40:9286–9297.
Zhao Y, Srivastava D. 2007. A developmental view of microRNA function. Trends Biochem Sci 32:189–97.
Zheng F, Liao YJ, Cai MY, Liu YH, Liu TH, Chen SP, Bian XW, Guan XY, Lin MC, Zeng YX, Kung HF, Xie D. 2012. The putative tumour suppressor microRNA-124 modulates hepatocellular carcinoma cell aggressiveness by repressing ROCK2 and EZH2. Gut 61:278–289.
Zhou J, Dong X, Zhou Q, Wang H, Qian Y, Tian W, Ma D, Li X. 2014. microRNA expression profiling of heart tissue during fetal development. Int J Mol Med 33:1250–1260.